A R C H I V E S O F M E T A L L U R G Y A N D M A T E R I A L S
Volume 60 2015 Issue 2
DOI: 10.1515/amm-2015-0253

M. MADEJ*,#

SOME ASPECTS OF INFILTRATION OF HIGH SPEED STEEL BASED COMPOSITES WITH IRON ADDITION

WYBRANE ZAGADNIENIA DOTYCZĄCE INFILTROWANYCH KOMPOZYTÓW STAL SZYBKOTNĄCA – ŻELAZO-MIEDŹ

Attempts have been made to describe the influence of the production process parameters and additions of iron powders on properties of copper infiltrated HSS based composites. The powder compositions used to produce skeletons for further infiltration were: M3/2, M3/2+20% Fe and M3/2+50% Fe. The powders were cold pressed at 800 MPa. The infiltration process was carried out in vacuum. Both green compacts and preforms sintered for 60 minutes at 1150°C in vacuum were contact infiltrated with copper to yield final densities exceeding 97% of the theoretical value.

The as-infiltrated composites were tested for Brinell hardness and bending strength, and subjected to wear tests performed by block-on-ring wear tester. From the analysis of the obtained results it has been found that the mechanical properties are mainly affected by the manufacturing route and composition of porous skeletons used for infiltration. Considerable differences in hardness between materials obtained from the two infiltration routes have been observed, with lower wear rates achieved after direct infiltration of green compacts.

Keywords: high speed steel, iron, composites, infiltration, tribological properties

Badania wykonano w celu określenia wpływu parametrów formowania i dodatku żelaza na własności infiltrowanych miedzią kompozytów na osnowie stali szybkotnącej z dodatkiem proszku żelaza. Zastosowano następujące mieszanki proszków do wytwarzania porowatych szkieletów przeznaczonych do infiltracji: M3/2, M3/2+20% Fe i M3/2+50% Fe. Mieszanki proszków prasowano pod ciśnieniem 800 MPa w matrycy o działaniu stempla jednostronnym bez zastosowania środków poślizgowych. Infiltrację prowadzono w próżni, w temperaturze 1150°C przez 15 minut. Jako porowate szkielety stosowano wypraski i spieki (60 minut w 1150°C w próżni). Infiltrację prowadzono metodą nakładkową.

Przeprowadzono badania twardości, wytrzymałości na zginanie oraz własności tribologicznych przy pomocy testera typu rolka -klocek. Wyniki jednoznacznie wskazują, że własności zależą zarówno od zawartości żelaza jak i technologii wytwarzania porowatych szkieletów przeznaczonych do infiltracji. Lepsze własności tribologiczne uzyskano dla infiltrowanych wyprasek. Mikrostruktura badanych kompozytów składa się z osnowy stali szybkotnącej, wydzieleń węglików typu MC oraz M_6C, żelaza oraz wydzieleń miedzi. Stwierdzono dyfuzję pierwiastków stopowych ze stali do żelaza.

1. Introduction

Some applications of PM tool steels are in circumstances where the priority is resistance to wear. Examples include cam followers, valve seat inserts, and oil pump components. An ability to press and sinter to near net shape requires good compressibility of the powder. High hardness, mechanical strength, heat resistance and wear resistance of M3/2 high speed steel (HSS) make it an attractive material for manufacture of valve train components [1÷8]. In this application, the material must exhibit resistance to oxidation, high hot strength and hardness, and superior wear resistance. Metal matrix composites could be produced by the infiltration technique. Since technological and economical considerations are equally important, infiltration of high-speed steel based skeleton with liquid cooper has proved to be a suitable technique whereby fully dense material is produced at low cost [1÷3, 5]. Low cost are also guaranteed by the addition of iron powder. An ability to press and sinter to near net shape requires good compressibility of the powder. Even after annealing, tool steel powders can be pressed to only about 80% of the theoretical density by most commercial facilities [6, 7,9]. On sintering and infiltration, little or no shrinkage can be tolerated and so the necessary strength and toughness may be achieved without removal of the remaining porosity. A reasonable compromise between all of these requirements may be achieved by using mixtures of high speed steel powders with softer low alloy or pure iron powder. During sintering and infiltration of such mixtures, interdiffusion of both carbon and metallic alloying elements occurs. In the particular case of copper infiltrated iron and steel compacts, the base iron matrix, or skeleton, is heated in contact with the copper alloy to a temperature exceeding the melting point of copper, normally to between 1095 and 1150°C.

* AGH-UNIVERSITY OF SCIENCE AND TECHNOLOGY, FACULTY OF METALS ENGINEERING AND INDUSTRIAL COMPUTER SCIENCE, AL. A. MICKIEWICZ 30, 30-059 KRAKÓW, POLAND
# Corresponding author: mmadej@agh.edu.pl

2. Experimental procedure

The Powdrex water atomised M3/2 grade HSS powder and Höganäs NC 100.24 iron powder, both finer than 160 μm, were used in the experiments. The HSS powder was delivered in as-annealed condition. Its chemical composition is given in Table 1, whereas its morphology and microstructure are shown in Figure 2.

TABLE 1
Chemical composition of M3/2 HSS powder, wt-%

C	Cr	Co	Mn	Mo	Ni	Si	V	W	O	Fe
1.23	**4.27**	**0.39**	**0.21**	**5.12**	**0.32**	**0.18**	**3.1**	**6.22**	**0.0626**	**balance**

Various amounts of iron were added to the HSS powder prior to compaction. The morphology of used powders are shown in Figure 1.

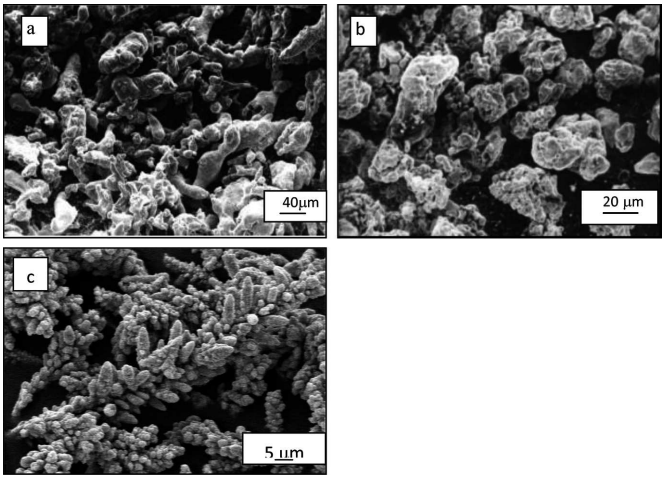

Fig. 1. SEM micrographs of: a) M3/2 HSS: b) NC 100.24 iron c) copper

The following compositions were investigated:
1. M3/2
2. M3/2 + 20 % Fe (wt%)
3. M3/2 + 50 % Fe (wt%)

The mixtures were prepared by mixing for 30 minutes in a Turbula®T2F mixer and cold pressed in a rigid cylindrical die at 800 MPa. There were two types of porous skeletons used for infiltration: green compacts and as-sintered compacts. The infiltration process was carried out in vacuum better than 10^{-3}Pa. Both green compacts and performs sintered for 60 minutes at 1150°C in vacuum were infiltrated with copper. Carefully pre-weighed pieces of copper infiltrant were placed on top of the rigid skeletons of predetermined porosity, heated to 1150°C, held at temperature for 15 minutes, and cooled down with the furnace to room temperature.

The infiltrated specimens were subsequently tested for Brinell hardness, bending strength and resistance to wear, and subjected to microstructural examinations by means of both light microscopy (LM) and scanning electron microscopy (SEM). The wear tests were carried out using the block-on-ring tester (Figure 2).

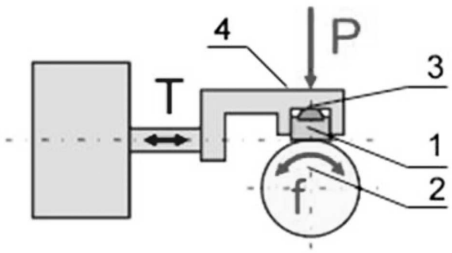

Fig. 2. Wear test principle on Tribosystem T05

During the test a rectangular wear sample (1) was mounted in a sample holder (4) equipped with a hemispherical insert (3) ensuring proper contact between the test sample and a steel ring (2) rotating at a constant speed. The wear surface of the sample was perpendicular to the loading direction. Double lever system was used to force the sample towards the ring with the load accuracy of ±1%.

The wear test conditions were:
- test sample dimensions: 20×4×4 mm,
- rotating ring: heat treated steel, 55 HRC, ø49,5×8 mm,
- rotational speed: 500 r/min,
- load: 165 N,
- sliding distance: 1000 m.

The measured parameters were:
- loss of sample mass,
- friction force F (used to calculate the coefficient of friction).

3. Results and discussion

3.1. Characterisation of the porous skeletons

The first step of the production process was to prepare a porous skeletons for infiltration process. There were two ways to produce its: compacting and compacting and sintering.

A fully-dense material made of the M3/2 grade powder can be achieved by sintering at around 1250°C [5], therefore to produce porous preforms the compacts were sintered at 1150°C. The combined effects of the powder mix composition and its processing route on relative densities of the porous skeletons are shown in Figure 3.

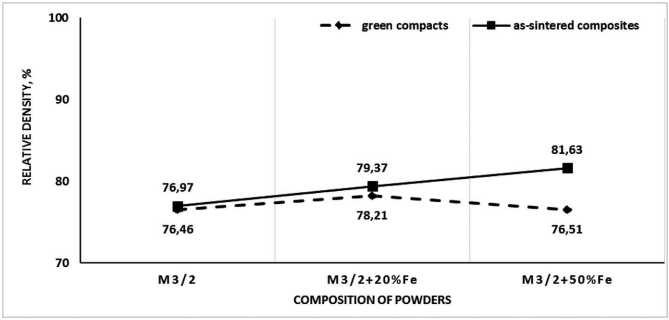

Fig. 3. Relative densities of green compacts and pre-sintered porous skeletons

From Figure 3 it is evident that the as-sintered densities of M3/2 are approximately equal to their green densities, whereas the addition of 20% iron to M3/2 has a negligible effect on

the as-sintered density. Relative density of samples obtained after pressing or after pressing and sintering allows the use of them as a porous skeletons for infiltration.

3.2. The properties of copper infiltrated HSS based composites

The properties of the as-infiltrated composites are shown in Figures 4÷11.

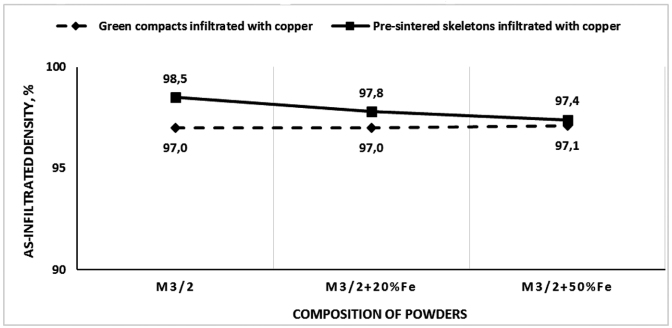

Fig. 4. Relative densities of as-infiltrated composites

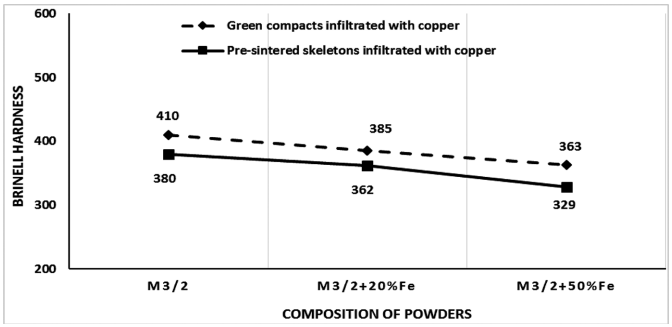

Fig. 5. The Brinell Hardness of as-infiltrated composites

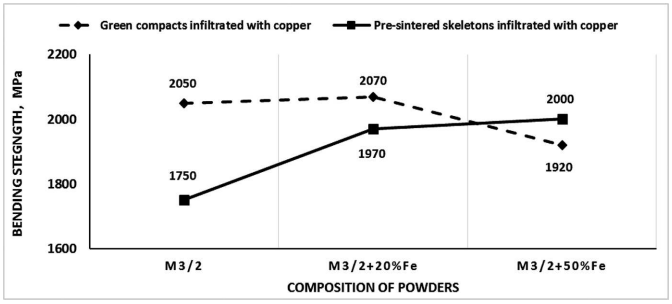

Fig. 6. The Bending Strength of as-infiltrated composites

As seen in Figure 4 the molten copper was drawn into the interconnected pores of the skeletons, through a capillary action, and filled virtually the entire pore volume to yield final densities exceeding 97% of the theoretical value. In the case of the addition of 20%, the Cu excess remains on the sample surface and is mechanically removed by brushing.

The Brinell hardness of the as-infiltrated composites decreases with the increased content of iron in the starting powder mix, whereas the bending strength does not seem to be affected. For pre-sintered samples an increase of bending strength occurs, this can be explained by the diffusion of carbon and alloying of iron particles during sintering. Substantial differences in hardness are observed between the materials obtained from the two infiltration routes. Markedly higher hardness numbers were achieved after direct infiltration of green compacts.

3.3. Tribological properties

The wear test results are given in Figures 7 and 8.

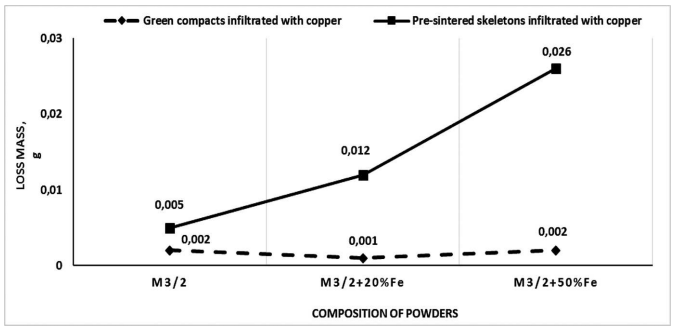

Fig. 7. Loss of mass of as infiltrated composites

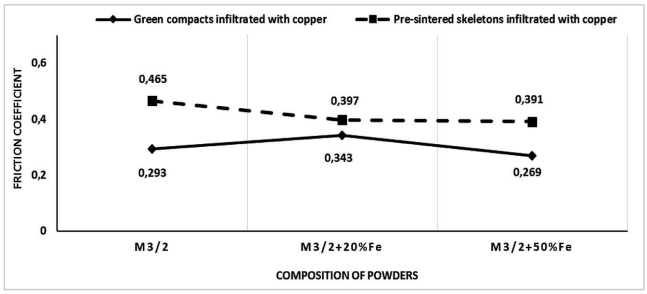

Fig. 8. Friction coefficient of as infiltrated composites

The measurements of the wear resistance and friction coefficient permit classification of the as-infiltrated composites with respect to their tribological properties. Direct infiltration of green compacts with copper results in the highest wear resistance and lower friction coefficient of the as-infiltrated M3/2, M3/2+20% Fe and M3/2+50% Fe composites. By comparing the wear resistance of composites received through direct infiltration of green compacts and infiltration of pre-sintered skeletons it is evident that the pre-sintered M3/2+Fe compositions show 12÷13 times higher loss of mass than the iron containing green compacts infiltrated with copper. This can be explained by the diffusion of carbon and alloying of iron particles during sintering.

Addition of 50% iron powder decreases the friction coefficient of composites received from direct infiltration of green compacts. It could be explained by the presence of iron inclusions in the microstructure of as-infiltrated composites, which impart good sliding properties.

Characteristic surface topographies after the wear test are exemplified in Figure 9.

The surface topographies of M3/2 and M3/2+50% Fe specimens indicate occurrence of different wear mechanisms (Figure 9). The carbides seen on the wear-surfaces are being crushed and pulled out of the matrix to act as abrasive particles which increase the coefficient of friction. Figure 9a provide evidence of ploughing and sideways displacement of

material in M3/2. Figure 9b shows smearing of iron over the surface of the as-infiltrated M3/2+50% Fe composite which implies marked contribution of adhesive wear, whereas the extensive formation of iron oxides may account for the lowest friction coefficients.

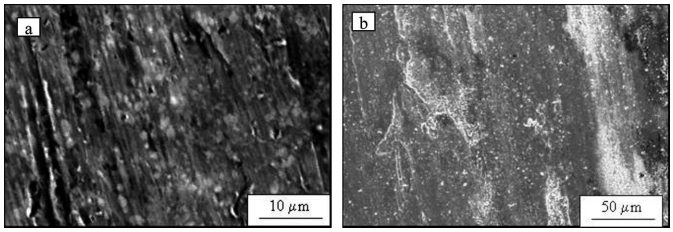

Fig. 9. The surface of the as-infiltrated composites after examining the wear resistance: a) M3/2, b) M50 % Fe

3.4. Microstructures

Typical microstructures of copper infiltrated green compacts and pre-sintered skeletons are shown in Figs 10÷12.

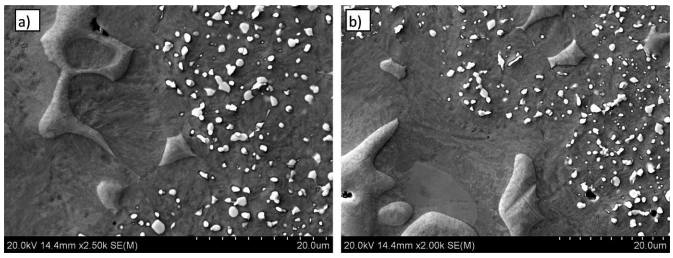

Fig. 10. Microstructures of M3/2 HSS based composites with 50% Fe additions: a) green compact infiltrated with copper, b) pre-sintered skeleton infiltrated with copper

It can be seen that the microstructure of the M3/2 grade HSS based composites with iron additions consists of a steel matrix with finely dispersed carbides, iron particles and islands of copper (Fig. 10). From the microstructural observations (Figs 10) it is also evident that the infiltration with copper almost completely eliminates porosity. Figs 11 show uniform distribution of carbides in the as-infiltrated microstructures of HSS matrix of the composites at the interface of HSS particles and copper particles.

It illustrates the existence of the main carbides M_6C and MC as well as the existence of ferrite and austenite in as-sintered matrix of HSS. Most Fe is found in the matrix and grey M_6C carbides, while W and V are found in the within MC carbides. The tribological properties of as-sintered and as-infiltrated composites M50Fe (Fig. 7) show that after infiltration of as-sintered porous skeletons it is observed that loss of mass was twelve times worse than in as-infiltrated green compact M50Fe. It can be explained by the diffusion of carbon and alloying elements from HSS matrix to iron particles during sintering which consequently leads to a reduction of matrix properties. The diffusion of alloying elements from steel matrix to iron particles during sintering process was analysed by SEM and EDX methods. Figure 12 shows linear analysis of distributions of elements at the interface of iron – copper – high speed steel particles in sintered and infiltrated M50Fe composites.

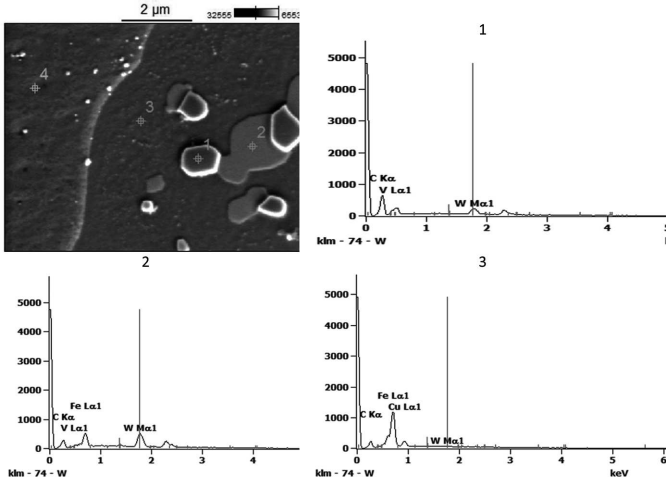

Fig. 11. SEM microstructure HSS matrix of sintered and infiltrated M3/2 composites: 1 – MC carbides, 2 – M_6C carbides, 3 – HSS matrix, 4 – copper

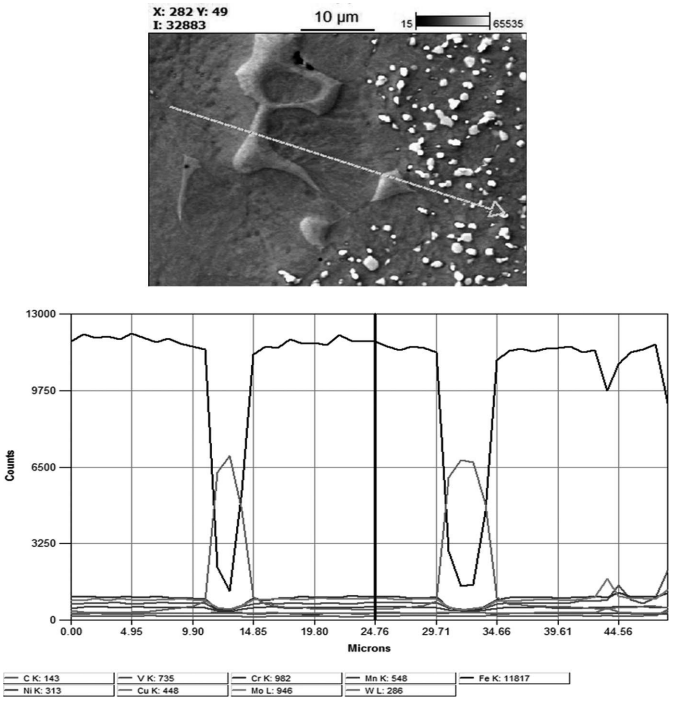

Fig. 12. The microstructure of HSS matrix and the qualitative EDX analysis:

It is known that after heating above 900°C the $M_{23}C_6$ carbide begins to dissolve and continues this up to temperature of 1100°C, but there is very small amount of $M_{23}C_6$ type of carbides in M3/2 HSS. The solution of M_6C carbides existing in M3/2 HSS begins at 1150°C, MC carbides barely dissolves at all. From Fig.12 it is evident that there is diffusion of carbon, chromium, molybdenum and manganese from steel to iron particles. This elements diffuse from high speed steel matrix and partially dissolved carbides M_6C type which were located near iron-high speed steel boundary. Diffusion of this elements during sintering of steel with iron addition is enhanced by the presence of carbon in solution [9], during sintering at temperatures 1150°C carbides dissolves and carbon diffuse to austenitic matrix of HSS and to iron particles.

There is also bidirectional diffusion from copper to iron and to HSS matrix.

In view of high cost of major alloying elements used in HSS the additions of iron powder to HSS seems to be good choice, this composite materials after infiltration could be used for non-cutting applications, where high strength is required without the need for large fraction of free carbides. The infiltration of copper to porous skeletons made of HSS + Fe give as better thermal conductivity properties.

4. Conclusions

The typical microstructure of high speed steel based composites infiltrated with copper with high iron content is composed of MC, M_6C, ferrite, tempered martensite residual austenite and copper regions. The mechanical properties of the HSS based composites are strongly dependent on the iron content. The additions of iron powders decrease the hardness of HSS based composites, but mostly increase their bending strength. The wear resistance of high speed steel with iron content depends on its additions volume. The pre-sintered, iron containing specimens show 12 times higher loss of mass than the iron containing green compacts infiltrated with copper, which have similar tribological properties to HSS infiltrated with copper composites.

Received: 20 February 2014.

Acknowledgements

This work was done in frame of the project No 11.11.110.299, which was financed by Ministry of Science and Higher Education.

REFERENCES

[1] G. Greetham, Powder Metallurgy **3**, 2, 112-114 (1990).
[2] R.H. Palma, The International Journal of Powder Metallurgy **37**, 5, 29-35 (2001).
[3] C.S. Wright, Powder Metallurgy **3**, 937-944 (1994).
[4] J. Leżański, The liquid infiltration in porous materials. Metalurgia i Odlewnictwo, 100-118, (1988) (in Polish).
[5] J.M. Torralba, State of the art. Powder Metallurgy Progress **36**, 55-66 (1993).
[6] P. Bała, J. Pacyna, Archives of Metallurgy and Materials **53**, 3, 795-801 (2008).
[7] B. Leszczyńska-Madej, Archives of Metallurgy **58**, 1, 43-48 (2013).
[8] M. Madej, Archives of Metallurgy and Materials **53**, 3, 839-845 (2008).
[9] N.A. Rhodes, J.V. Wood, J.R. Moon, Powder Metallurgy **43**, 2, 157-162 (2000).